

ARTICLE OPEN



Characterization and genome analysis of a psychrophilic methanotroph representing a ubiquitous *Methylobacter* spp. cluster in boreal lake ecosystems

Ramita Khanongnuch¹ , Rahul Mangayil¹, Mette Marianne Svenning² and Antti Juhani Rissanen^{1,3} 

© The Author(s) 2022

Lakes and ponds are considered as a major natural source of CH₄ emissions, particularly during the ice-free period in boreal ecosystems. Aerobic methane-oxidizing bacteria (MOB), which utilize CH₄ using oxygen as an electron acceptor, are one of the dominant microorganisms in the CH₄-rich water columns. Metagenome-assembled genomes (MAGs) have revealed the genetic potential of MOB from boreal aquatic ecosystems for various microaerobic/anaerobic metabolic functions. However, experimental proof of these functions, i.e., organic acid production via fermentation, by lake MOB is lacking. In addition, psychrophilic (i.e., cold-loving) MOB and their CH₄-oxidizing process have rarely been investigated. In this study, we isolated, provided a taxonomic description, and analyzed the genome of *Methylobacter* sp. S3L5C, a psychrophilic MOB, from a boreal lake in Finland. Based on phylogenomic comparisons to MAGs, *Methylobacter* sp. S3L5C represented a ubiquitous cluster of *Methylobacter* spp. in boreal aquatic ecosystems. At optimal temperatures (3–12 °C) and pH (6.8–8.3), the specific growth rates (μ) and CH₄ utilization rate were in the range of 0.018–0.022 h⁻¹ and 0.66–1.52 mmol l⁻¹ d⁻¹, respectively. In batch cultivation, the isolate could produce organic acids, and the concentrations were elevated after replenishing CH₄ and air into the headspace. Up to 4.1 mM acetate, 0.02 mM malate, and 0.07 mM propionate were observed at the end of the test under optimal operational conditions. The results herein highlight the key role of *Methylobacter* spp. in regulating CH₄ emissions and their potential to provide CH₄-derived organic carbon compounds to surrounding heterotrophic microorganisms in cold ecosystems.

ISME Communications; <https://doi.org/10.1038/s43705-022-00172-x>

INTRODUCTION

Methane (CH₄) is one of the major natural and anthropogenic greenhouse gases, with a global warming potential of approximately thirty times higher than that of CO₂ over a 100-year time horizon [1]. Lakes, one of the major natural sources of CH₄ emissions, have recently gained interest as they account for ~6–7% of the total natural emissions [2, 3]. In particular, the emissions from boreal and arctic lakes are elevated during the ice-free period than at other times of the year [3–6].

In the lake ecosystems, CH₄ is generally produced by methanogenic archaea in anoxic sediments/layers and eventually emitted upwards toward the water-atmosphere interface. During CH₄ traveling along the lake water column, various studies have reported the function of aerobic methane-oxidizing bacteria (MOB) as the key factor in controlling these CH₄ fluxes at the oxic-anoxic interfaces in boreal and arctic lake ecosystems [7–11]. MOB require oxygen as an electron acceptor to oxidize CH₄ for biomass formation and CO₂ generation. During hypoxic (i.e., oxygen-limiting) conditions, MOB may shift the cellular metabolism toward fermentation to stabilize their cellular redox potential, either by generating various extracellular organic acids [12] or using nitrate as the terminal electron acceptor via anaerobic respiration [13]. The metabolism of MOB is of great ecological importance as the produced by-products (e.g.,

methanol, formaldehyde, and organic acids) can serve as growth substrates for surrounding methylotrophic and heterotrophic microorganisms [14, 15]. Furthermore, MOB interacting with a high heterotroph richness in a coculture system could also enhance CH₄ oxidation as the cross-feeding mechanism might help to reduce the toxic compounds' inhibitory effect on MOB [14]. Studies on implementing the produced extracellular by-products as biofuel precursors or as industrial platform chemicals also imply the biotechnological importance of MOB [16–18].

The study of metagenome-assembled genomes (MAG) and experimental observations have revealed that MOB in northern lakes have the genetic potential for denitrification and fermentation, resulting in organic acid production [7, 19]. During our previous study on genomic characteristics of boreal lake water column MOB, an attempt to demonstrate organic acid production by MOB in northern lakes was conducted via experimental incubation of natural lake water samples [7]. However, it was not successful due to the low concentrations of organic acids (results not shown in [7]). This suggests that the study on fermentation by lake MOB requires the cultivation of enrichment or obtaining isolates of lake MOB. Up to now, CH₄ oxidation metabolism in cold conditions, including psychrophilic conditions (0–20 °C), has rarely been studied using enrichment or isolates of MOB [20, 21].

¹Faculty of Engineering and Natural Sciences, Tampere University, P.O. Box 541, 33014 Tampere, Finland. ²Department of Arctic and Marine Biology, UiT, The Arctic University of Norway, 9037 Tromsø, Norway. ³Natural Resources Institute Finland, Latokartanonkaari 9, 00790 Helsinki, Finland. ✉email: ramita.khanongnuch@tuni.fi; antti.rissanen@tuni.fi

Received: 31 May 2022 Revised: 31 August 2022 Accepted: 6 September 2022

Published online: 19 September 2022

The study on lake MOB isolates would benefit in understanding their function, environmental distribution, and potential to broaden the biotechnological prospects of MOB. Herein, we focused on isolation, characterization, whole genome assembly, and evaluation of organic acid production of a psychrophilic MOB strain isolated from a boreal lake.

MATERIALS AND METHODS

Sampling site

Lake water samples from a small humic and O₂-stratified lake, Lake Lovojärvi in southern Finland (61° 04'N, 25° 02'E), were used as the isolation source [22]. The sampling was conducted at the hypoxic layer (5.75 m depth, temperature 5.2 °C, pH 6.5, and dissolved O₂ concentration (DO) < 0.3 mg l⁻¹) (Supplementary Fig. S1). Lake water samples were pre-filtered through a 50 µm mesh to remove larger plankton. The filtered water was collected in 250 ml glass bottles containing 20% CH₄ and 80% air (v/v) and stored at 5 °C prior to enrichment.

Enrichment and isolation

In this study, nitrate mineral salts (NMS) medium modified from DSMZ medium 921 with an initial pH of ~6.80 (Supplementary Table S1) was used as the liquid growth medium of MOB. The solid medium consisted of the NMS liquid medium supplemented with 1.5% Noble agar (Agar-Agar SERVA powder analytical grade, Germany). For MOB enrichment, 0.5 ml lake water was added into a 25 ml sterile serum bottle containing a 5 ml sterile NMS medium. The bottle was sealed with sterile butyl rubber stoppers and aluminum crimps, and the headspace was replaced with 20% (v/v) of CH₄ prior to incubating in static conditions at 5 °C for 42 days. The enriched culture was sub-cultured thrice in the NMS medium prior to streaking onto the NMS agar medium. Agar plates were incubated in an air-tight chamber containing ~20% CH₄ and 80% air (v/v) in the headspace and placed at 5 °C for ~60 days. Colonies were picked under a stereo microscope and re-streaked onto NMS agar medium. Heterotroph contamination was checked by streaking colonies on nutrient-rich agar medium (0.5% tryptone, 0.25% yeast extract, 0.1% glucose and 2% agar). Culture purity was confirmed when one cell type was observed under a light microscope, and growth was absent on both nutrient-rich and NMS media without CH₄ supplementation. The culture purity was also confirmed by high-throughput full-length 16S rRNA gene amplicon sequencing using the Pacbio Sequel platform (Novogene Co. Ltd., Beijing, China).

Biochemical characterization

The growth tests at different pH, temperatures, and nitrogen sources were conducted in 27 ml sterile glass tubes containing 5 ml NMS medium and an initial culture of optical density at 600 nm wavelength (OD_{600nm}) of 0.02. The tubes were subsequently sealed with sterile butyl rubber stoppers and aluminum crimps. The initial headspace gas composition of 20% CH₄ and 80% air (v/v) was established by replacing 20% (v/v) of the air headspace with pure CH₄. The pH test was performed in triplicates (pH 4.7–8.3) at 5 °C under static conditions. The growth temperature test was conducted in duplicate using a temperature-gradient incubator (Terratec Corporation, Hobart, Australia), set in the range of 0–26 °C (at pH 6.8). In the different nitrogen source tests, NMS and ammonium mineral salts (AMS) media (Supplementary Table S1) were used as nitrate and ammonium sources, respectively, to cultivate the isolate. The test was conducted in duplicate. In addition, the total cellular carbohydrate content during the growth in NMS and AMS media was measured at the end of the test. All tests were incubated at static conditions for ~19–21 days. CH₄ and CO₂ compositions in the headspace and OD_{600nm} were monitored daily during weekdays, while O₂ in the headspace and organic acid concentrations in the liquid medium were measured at the beginning and end of the test. The growth rates (µ) were obtained from linear regression of the plot between Log₁₀ optical density versus incubation time. To test nitrogen (N₂) fixation, the isolate was incubated in 25 ml serum bottles containing sterile nitrate free-NMS liquid medium. The headspace (v/v) was supplemented with (i) 20% CH₄ + 80% N₂ and (ii) 20% CH₄ + 5% O₂ + 75% N₂ for anaerobic and microaerobic conditions, respectively. The bottles were sealed with sterile butyl rubber stoppers with aluminum crimps and incubated statically at ~5 °C for over 30 days.

DNA extraction and identification

Genomic DNA (gDNA) extraction was performed using GeneJET genomic DNA purification kit (Thermo Fisher Scientific, USA). The gDNA was quantified using a Qubit 3.0 Fluorometer and a dsDNA HS Assay Kit (Thermo Fisher Scientific, USA). PCR and amplicon sequencing (Sanger Sequencing method) of the 16S rRNA gene were performed using the identification service offered by Macrogen (Amsterdam, The Netherlands), using primer pairs 27F (AGAGTTTGATCMTGGCTCAG) and 1492R (TACGGY-TACCTTGTACGACTT) for amplification and primer pairs 785F (GGATTA-GATACCCTGGTA) and 907R (CCGTCATTCMTTTRAGTTT) for sequencing. A 16S rRNA gene-based phylogenetic tree was constructed in Mega X using the maximum-likelihood algorithm (generalized time-reversible model) with 100 bootstraps [23]. Besides reference strains, the tree was supplemented with 16S rRNA gene sequences of previously studied environmental MAGs representing *Methylobacter* spp. of lakes and ponds of boreal, subarctic, and temperate areas [24, 25]. For the dataset on multiple lakes and ponds, we chose the representative MAGs of metagenomic Operational Taxonomic Units [mOTUs, classified by Buck et al. [24] at 95% average nucleotide identity cutoff]. The 16S rRNA genes were extracted from MAGs using barnap (version 0.9) [26].

Genome sequencing, assembly, and annotation

Library preparation and sequencing for long reads (PacBio Sequel SMRT Cell 1M v2) and short reads (Illumina NovaSeq 6000 platform) were done by Novogene Co. Ltd. (Beijing, China) as previously described by Rissanen et al. [22]. The genomes were de novo assembled using a hybrid assembly strategy in Unicycler (version 0.4.8) with default parameters and “-mode normal” [27]. The assembled genome was annotated using the NCBI Prokaryotic Genome Annotation Pipeline [28–30]. Key functional genes and metabolic pathways of the annotated genome were also predicted and reconstructed using Kyoto Encyclopedia of Genes and Genomes (KEGG) mapping tools [31] with KofamKOALA (<https://www.genome.jp/tools/kofamkoala/>; accessed 1 February 2022) [32].

The genome-wide phylogenetic tree was built from protein alignments generated in PhyloPhlAn (version 3.0.58; PhyloPhlAn database including 400 universal marker genes and “-diversity low” - argument) [33] using the maximum-likelihood algorithm (PROTCATLG – model) with 100 bootstrap replicates in RAXML (version 8.2.12) [34]. Similar to 16S rRNA gene-based phylogenetic tree analysis as explained above, this analysis was supplemented with environmental MAGs representing *Methylobacter* spp. from lakes and ponds of boreal, subarctic, and temperate areas [24, 25], as well as from temperate wetland [10]. The MAGs were also functionally annotated using Prokka (version 1.13.3) [35] and KofamKOALA, as explained above [32]. Average nucleotide identities (ANI) of the genome with the reference genomes and MAGs were computed using fastANI (version 1.32) [36], while average amino-acid identity (AAI) was calculated using CompareM (version 0.1.2) (<https://github.com/dparks1134/CompareM>). Digital DNA-DNA hybridization (dDDH) for genome-based taxonomic classification was calculated using the Type Strain Genome Server (TYGS) online service (<https://tygs.dsmz.de/>; accessed 28 February 2022) [37]. Furthermore, *pmoA* sequences coding for the beta subunit of particulate methane monooxygenase of the MAGs, genome, and reference genomes were subjected to phylogenetic tree analyses using the neighbor-joining method (Jones-Taylor-Thornton model) with 500 bootstraps in Mega X [23].

Evaluation of organic acid production by the isolate

The organic acid production potential of the isolate was evaluated in batch experiments performed in 120 ml sterile serum bottles. Prior to sealing with sterile butyl rubber stoppers and aluminum crimps, 15 ml of NMS medium (pH 6.8) was added to the bottles. The initial culture inoculated into the medium and CH₄ concentration in the headspace were previously described in Section *Biochemical characterization*. The experiment was conducted in six bottles and incubated at 10.0 ± 1.0 °C in static conditions for 20 days. On day 20, the experiment was divided into two sets, including the first set (in triplicates) replenished with 20% CH₄ + 80% air (v/v) in the headspace, whereas another set (in triplicate) was used as a control without replenishment. The incubation was subsequently continued under similar conditions until day 33. In this study, organic acid production, OD_{600nm}, pH in the liquid medium, and the gas composition in the headspace were periodically monitored every 2 or 3 days. However, in the control test without the replenishment, the gas composition in the headspace was monitored only at the beginning and end of the

experiment. NMS medium without cells and an inoculated culture without CH₄ and air addition were also used as controls.

Analytical methods

Cell growth was determined using an Ultrospec 500 pro spectrophotometer (Amersham Biosciences, UK). The medium pH was measured using a pH 330i portable meter (WTW, Germany) equipped with a SlimTrode electrode (Hamilton, Germany). To determine the organic acid composition, the cultures centrifuged (15 min at 2700 × g) and filtered through a 0.2 μm membrane (Chromafil[®] Xtra PET 20/25, Macherey-Nagel, Germany) were analyzed using a Shimadzu high-performance liquid chromatography equipped with Rezex RHM-Monosaccharide H⁺ column (Phenomenex, USA) as described in Okonkwo et al. [38]. Gas composition in the headspace (i.e., CH₄, CO₂, and O₂) was measured using a Shimadzu gas chromatograph GC-2014 equipped with a thermal conductivity detector and a Carboxen-1000 60/80 column (Agilent Technologies, USA) as described in Khanongnuch et al. [16]. To obtain further insight into the distribution of carbon in the cell biomass, the total carbohydrate content was evaluated using the phenol-sulfuric acid method [39]. The standard curve of the test was prepared using known glucose concentrations.

Statistical analysis

The specific growth rate, CH₄ utilizing rate, and organic acid concentration from different experimental conditions were statistically compared using one-way analysis of variance (ANOVA) (Minitab16.0, USA) with Tukey's multiple comparison tests. The significance level was the 95% confidence interval, where a *p* value ≤ 0.05 was considered statistically significant.

RESULTS

Isolation, characterization, and classification

The isolate was obtained from a single colony forming on NMS agar media after being incubated statically at ~5 °C for over 60 days. The isolate colonies were tiny, < 0.1 mm in diameter, cream, round and entire (Supplementary Fig. S2a). The cells were small and non-motile cocci (1.0–1.8 μm in diameter) that reproduced by binary fission (Supplementary Fig. S2b).

For 16S rRNA gene-based identification, the isolate showed 99.5% and 98.9% similarity to *Methylobacter psychrophilus* Z-0021 and *Methylobacter tundripaludum* SV96 isolated from tundra soil [40] and arctic wetland soil [41], respectively (Fig. 1; Supplementary Table S2). The strain formed a separate cluster in the 16S rRNA gene tree with *M. psychrophilus* and MAGs representing MOB from

lakes and permafrost thaw ponds (Fig. 1). The isolate was classified in the class *Gammaproteobacteria*, order *Methylococcales*, the family *Methylococcaceae*, and genus *Methylobacter*. Based on the *pmoA* gene-based analysis, the isolate was closely clustered with *M. psychrophilus* and MAGs representing MOB in boreal lake ecosystems (Supplementary Fig. S3).

Table 1 shows the characteristics of *Methylobacter* sp. S3L5C compared to other psychrophilic and psychrotolerant methanotrophic species. During the cultivation, *Methylobacter* sp. S3L5C grew only in the presence of CH₄ and O₂. Growth was not observed in the N₂-fixation test or under anaerobic conditions, but the cells were still viable in those conditions, even after over 1 year of incubation. The strain grew well at 3–12 °C, but the cell growth was not observed above 20 °C, demonstrating its psychrophilic nature (Fig. 2a, b). *Methylobacter* sp. S3L5C could grow well in the pH range of 6.0–8.3, and cell growth was not observed at pH 4.6 (Fig. 2d). At the optimal temperatures (3–12 °C) and pH (6.8–8.3), the specific growth rates (μ) and CH₄ utilization rate were in the range of 0.018–0.022 h⁻¹ and 0.66–1.52 mmol l⁻¹ d⁻¹, respectively (Fig. 2a, b, d, e). Formate (0.04–0.30 mM) and acetate (0.01–0.24 mM) were identified as the major liquid metabolites in all the tested conditions where the strain growth was present (Fig. 2c, f). The trend of acetate production showed that the increased concentration corresponded with the increase in cell growth (Fig. 2c, f).

Methylobacter sp. S3L5C could utilize both nitrate and ammonium as the nitrogen source. The specific growth rate in the AMS medium (μ = 0.040 h⁻¹) was higher than in the NMS medium (μ = 0.020 h⁻¹), whereas the CH₄ utilization rate was similar in both NMS and AMS media (0.52–0.88 mmol l⁻¹ d⁻¹) (Fig. 3a, b). In the case of liquid metabolites, acetate and formate were present in the NMS medium; however, only acetate was detected from the cultivations in the AMS medium (Fig. 3c). Furthermore, the total carbohydrate content in biomass cultivated in the NMS medium was 0.91 ± 0.04 mM glucose equivalent which was significantly higher than in the AMS medium (0.31 ± 0.09 mM glucose equivalent) (*p* value < 0.001) (Fig. 3d).

Genome features of *Methylobacter* sp. S3L5C

Methylobacter sp. S3L5C genome contained a single chromosome of 4,815,745 bp (G + C content, 43.3%) consisting of 4176 protein-

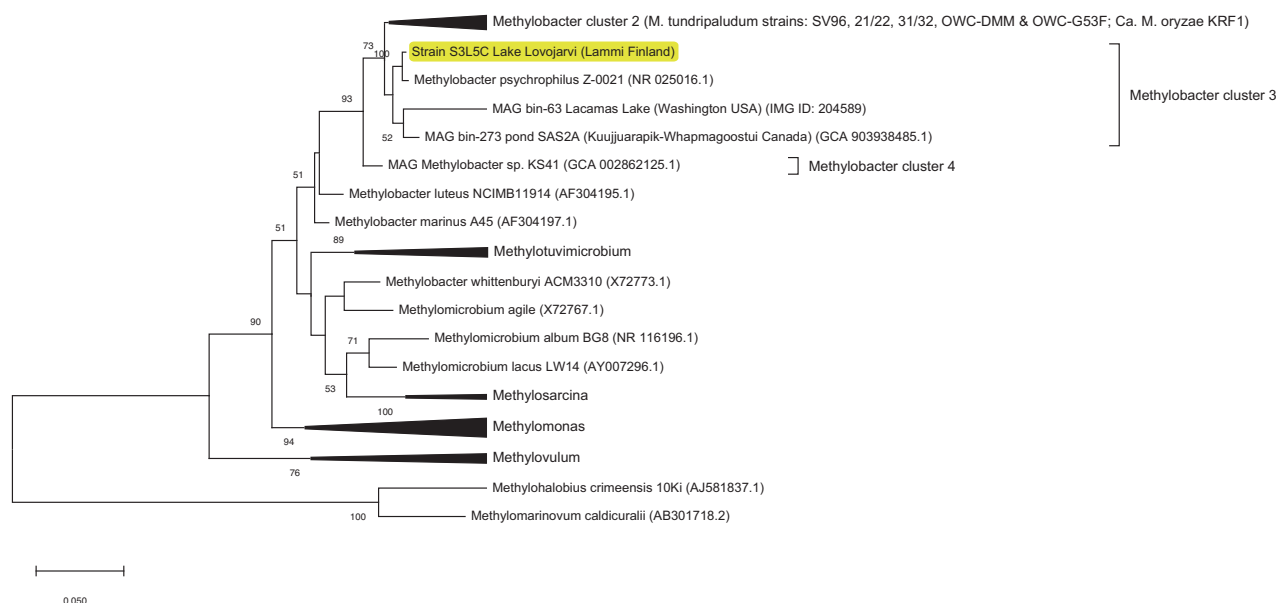
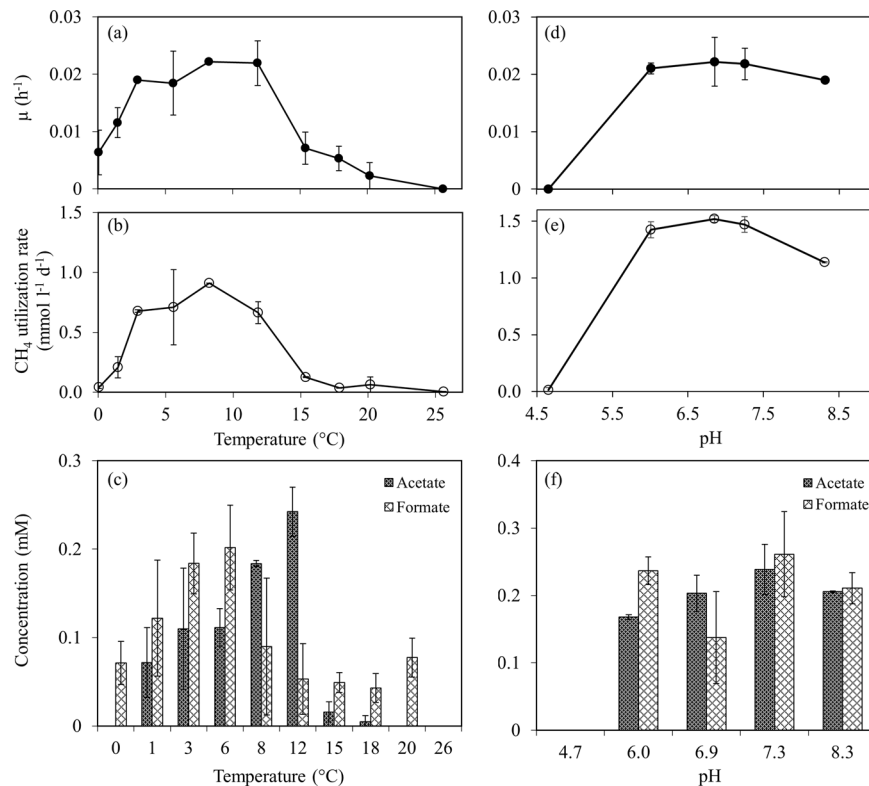


Fig. 1 A 16S rRNA gene-based phylogenetic tree of strain S3L5C. The tree shows the position of 16S rRNA gene of strain S3L5C (highlighted in yellow) compared with other pure culture methanotrophic bacteria and metagenome-assembled genomes (MAG). GenBank accession numbers are given in parentheses, and the bar shows a 5% sequence divergence.

Table 1. Characteristics of different psychrophilic and psychrotolerant species of methanotrophs.

Strain	<i>Methylobacter</i> sp. S3L5C	<i>Methylobacter psychrophilus</i> Z-0021	<i>Methylobacter tundripaludum</i> SV96	<i>Methylosphaera hansonii</i>
Source/habitat	Lake water layer	Tundra soil	Arctic wetland soil	Sediments of marine-salinity Antarctic meromictic lakes
Cell morphology	Cocci	Cocci	Rods	Cocci
Cell size (μm)	1.0–1.8	1.0–1.7	0.8–1.3 \times 1.9–2.5	1.5–2.0
Motility	–	–	–	–
Pigmentation	–	–	Pale Pink	NA
Growth pH	6.0–8.3	5.9–7.0	5.5–7.9	NA
(optimal)	(6.0–7.3)	(6.7)		
Growth temp. (optimal) ($^{\circ}\text{C}$)	0.1–20 (8–12)	1–20 (10)	5–30 (23)	0–21 (10–13)
Specific conditions for growth	–	–	–	Required seawater
Nitrogen fixation gene (<i>nif</i>)	+	NA	+	+
G + C content (mol %)	43.3	45–46 ^a	47	43–46 ^a
Reference	This study	[40]	[41]	[68]

NA not available.

^aG + C content was chemically determined as its genome is not available.**Fig. 2** Characterization of strain S3L5C growth at different temperatures and pH. (a, d) Specific growth, (b, e) CH₄ utilization rate, and (c, f) organic acid concentrations of strain S3L5C at the end of the tests at different temperatures (a–c) and pH (d–f). Error bars indicate the standard deviation of duplicates and triplicates for temperature and pH tests, respectively (See Supplementary Table S7 for the dataset).

coding sequences, five copies of rRNA (5S, 16S, 23S rRNA), 50 tRNA genes and 2 CRISPR sequences. *Methylobacter* sp. S3L5C genome was clustered together with MAGs of MOB from lakes and ponds in Finland, Sweden, the USA, Switzerland, and Canada (Fig. 4). Compared to available genomes of other methanotrophic isolates, the S3L5C genome formed a separate species-level branch, and it

was not represented by the other isolates (Fig. 4). Regarding similarity indexes for genomic comparison between the SL35C and other MOB, the dDDH was < 25%, while the ANI and AAI values were < 85% (Supplementary Table S3). To recognize the genomic uniqueness of a novel species, same-species delineation thresholds are recommended to be above 70% for dDDH, 95% for

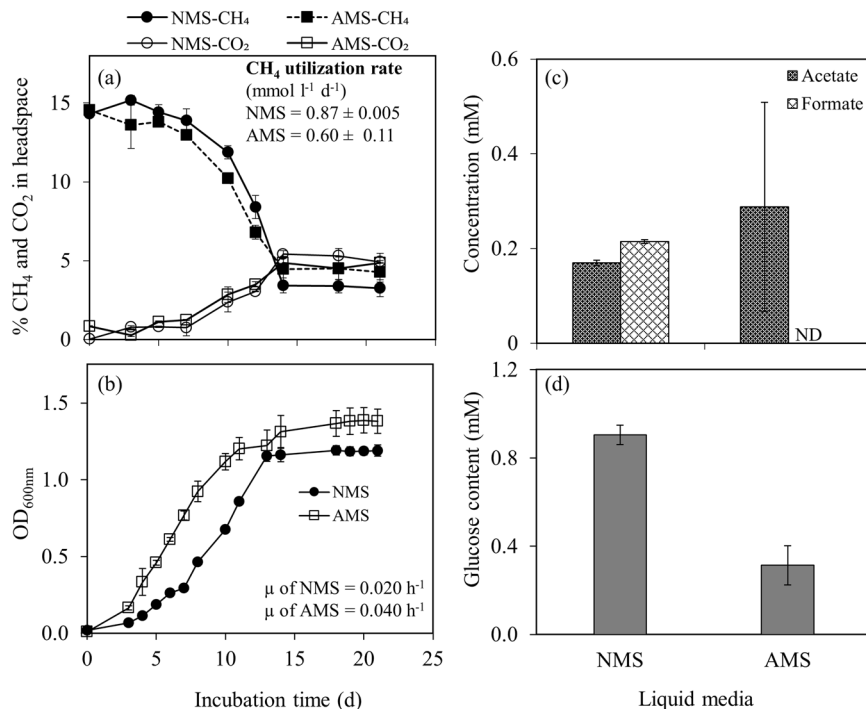


Fig. 3 Characterization of strain S3L5C growth with different nitrogen sources. Profiles of (a) CH₄ utilization and CO₂ production and (b) biomass growth during 21-day incubation in nitrate (NMS) and ammonium (AMS) mineral salt media. (c) Organic acid production and (d) glucose (representing carbohydrate) content of biomass measured at the end of the test (day 21). Error bars indicate the standard deviation of duplicate samples (See Supplementary Table S8 for the dataset).

ANI, 85% for AAI, and 98.7% similarity with 16S rRNA gene sequences [42–47]. Albeit the high sequence similarity of 16S rRNA genes between *Methylobacter* sp. S3L5C and *M. psychrophilus* Z-0021 (99.5% similarity), we could not confirm whether the strains represented identical species due to the non-existence of genome data of *M. psychrophilus* Z-0021. The latter strain is neither available in the DSMZ repository nor in the All-Russia Collection of Microorganisms (VKM B-2103) culture collection resource (last checked on 24 May 2022), where it was originally deposited [40, 41].

Predicted metabolic pathways

The key metabolic pathways in *Methylobacter* sp. S3L5C were predicted based on the KEGG database (Fig. 5). *Methylobacter* sp. S3L5C genome contains all key genes associated with CH₄ oxidation, including both particulate (*pmoCAB*) and soluble (*mmoXYBZDC*) methane monooxygenases. For the conversion of methanol to formaldehyde, the strain contained both calcium- (*mxoFJGIACKLD*) and lanthanide-dependent (*oxoF*) methanol dehydrogenases. Genes encoding tetrahydromethanopterin (H₄MPT)-mediated pathway, catalyzing the conversion of formaldehyde into formate, were present in the isolate. *Methylobacter* sp. S3L5C contained a complete set of genes encoding major pathways for formaldehyde assimilation into cell biomass, including ribulose monophosphate (RuMP), Embden-Meyerhof-Parnas (EMP), Enter-Doudoroff (EDD), and phosphoketolases (*xfp*)-based pathways (Fig. 5; Supplementary Table S4). The strain lacked the gene encoding serine-glyoxylate aminotransferase (*sga*), leading to the incomplete serine pathway. Genes present in *Methylobacter* sp. S3L5C also encoded the oxidative tricarboxylic acid (TCA) cycle and C5-branched dibasic acid metabolism.

Gammaproteobacterial MOB can generally oxidize NH₄⁺ into hydroxylamine (NH₂OH) using *pmoCAB* [48]. Our experimental observation suggests that the same NH₄⁺ metabolism might also occur in *Methylobacter* sp. S3L5C. However, the latter did not contain putative *hao* genes encoding hydroxylamine oxidoreductase to convert hydroxylamine to nitrite or nitric oxide [49]. The

genome also included nitrate/nitrite conversion genes, i.e., assimilatory nitrate reductase (*nasA*) for reducing nitrate into nitrite and nitrite reductase (*nirBD* and *nirS*) for reducing nitrite into ammonia and nitric oxide. Genes encoding nitrogen fixation (*nifHDK*) were found, although the CH₄ oxidation and growth were not observed in the culture-dependent experiments of nitrogen fixation under anaerobic and microaerobic (5% O₂) conditions.

Genes encoding the key enzymes involved in fermentative metabolisms were observed in the genome, including acetyl-CoA synthetase (*acdAB*) catalyzing the conversion of acetyl/propionyl-CoA into acetate/propionate and acetate kinase (*ackA*) for propionate generation from propionyl phosphate. However, some key genes involving acetate synthesis pathways, such as phosphate acetyltransferase (*pta*) and pyruvate dehydrogenase (*poxB*), were not present in the genome. The genome also included malate dehydrogenase (*mdh*) encoding the reversible conversion of oxaloacetate, succinate dehydrogenase (*sdhCDAB*) coupling with succinate production, and NAD⁺-reducing hydrogenase (*hoxFGYH*) encoding H₂ production. Based on further analyses of environmental MAGs, the similar genetic potential for fermentation and organic acid production is widely dispersed in closely related *Methylobacter* spp. of lakes, ponds, and wetlands of temperate and boreal areas (Supplementary Table S5).

Organic acid production potential

Batch cultivations were performed to evaluate the strain's potential to produce organic acids by replenishing CH₄ and air during incubation (on day 20, Fig. 6a). In the CH₄ + air replenishment test, the average utilized oxygen-to-methane (O₂/CH₄) molar ratio was 1.0 ± 0.5 mol mol⁻¹ during cultivation from days 4 to 33 (Supplementary Fig. S4). At the end of the test (day 33), the culture with the replenished headspace had utilized CH₄ and O₂ concentrations at ~1.5–2 times higher than those of the control cultivations without the replenishment, corresponding with the higher CH₄ and O₂ concentrations fed into the system (Supplementary Fig. S5a). On day 33, the CH₄ + air replenishment also increased the biomass

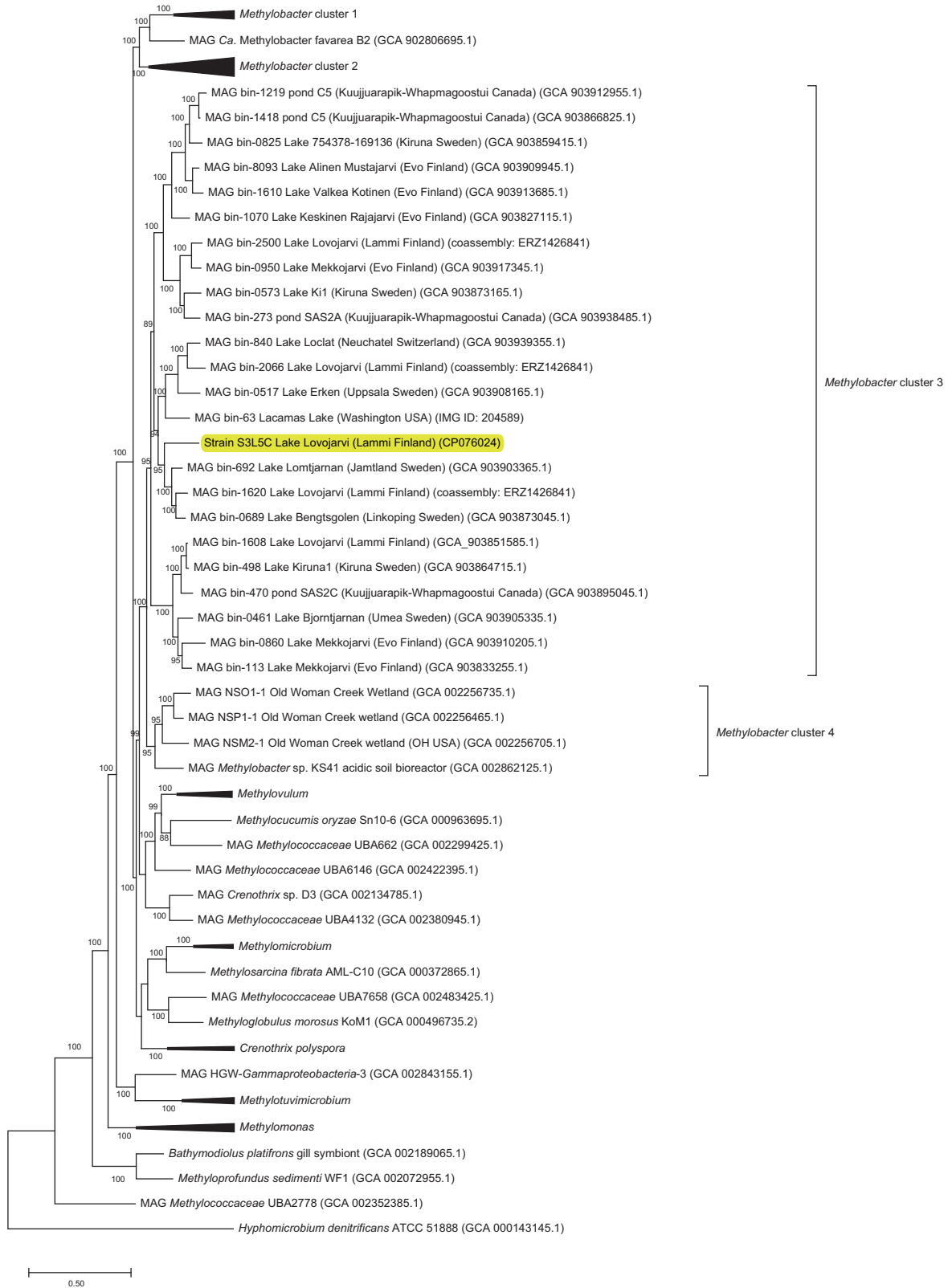


Fig. 4 Genome-wide phylogenomic tree of strain S3L5C. The tree was constructed using PhyloPhlAn2 showing the position of strain S3L5C (highlighted in yellow) compared to other cultured methanotrophs and metagenome-assembled genomes (MAGs) of uncultured *Methylobacter* and *Methylococcales* from environmental samples. *Methylobacter* clusters 1 and 2 contain the so far cultured members of *Methylobacter* spp.

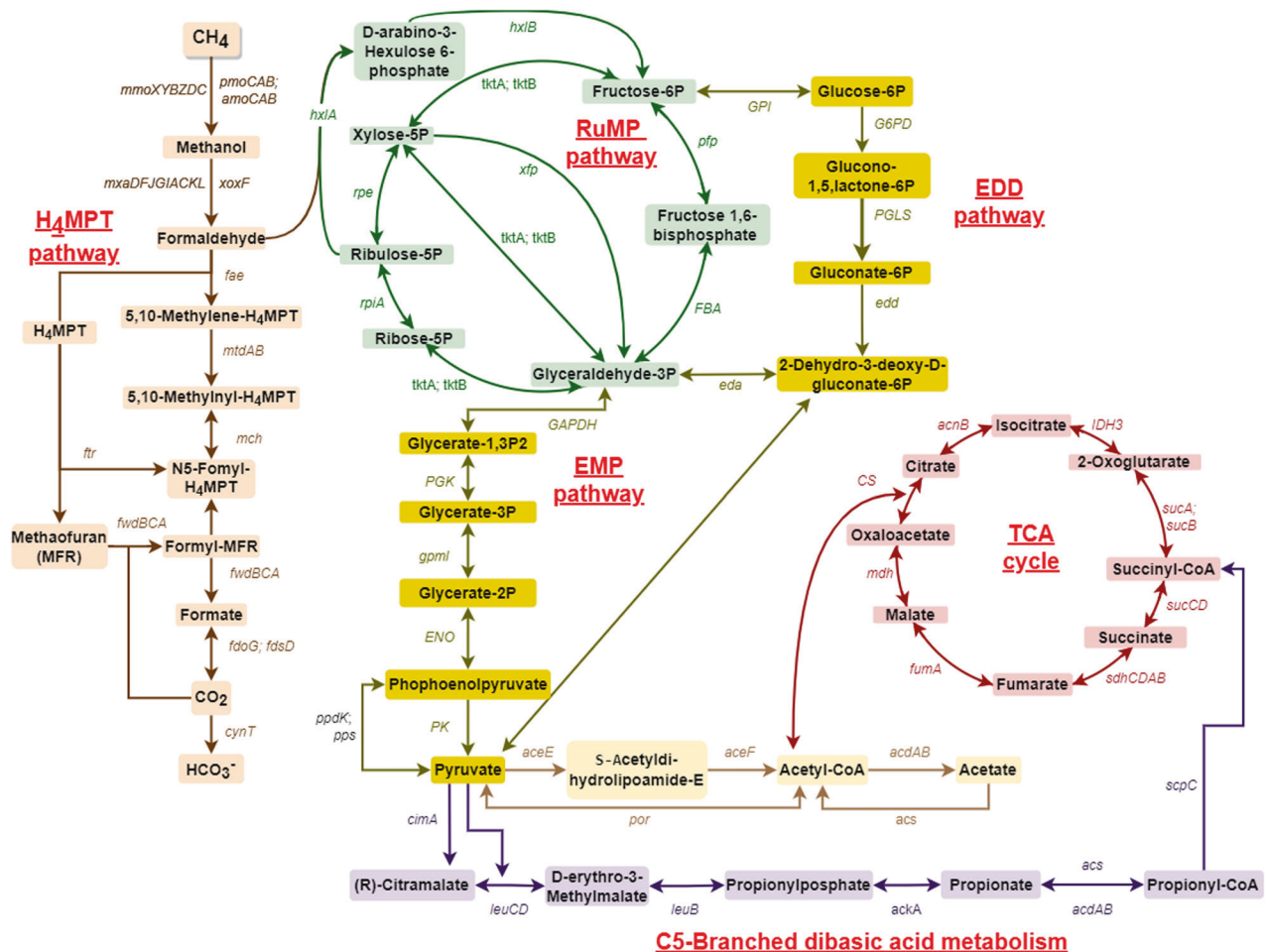


Fig. 5 Predicted metabolic pathway of *Methylobacter* sp. S3L5C constructed based on the KEGG mapper [31]. A list of genes is present in Supplementary Table S4. H₄MPT tetrahydromethanopterin, RuMP ribulose monophosphate, EMP Embden-Meyerhof-Parnas, EDD Enter-Doudoroff, TCA tricarboxylic acid.

growth (up to OD_{600nm} 5.0 ± 0.2), while an OD_{600nm} of 3.2 ± 0.4 was obtained in the control cultivations without CH₄ + air replenishment (Supplementary Fig. S5b).

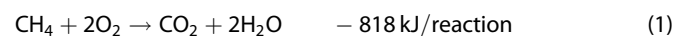
Acetate, formate, and malate were observed as soluble metabolites from *Methylobacter* sp. S3L5C cultivations with and without the replenishment, while propionate was only present in the test with CH₄ + air replenishment (Fig. 6b). Organic acid concentrations gradually accumulated during the cultivation period, except for formate, which was mostly depleted in both experimental conditions (Fig. 6b, c). In the tests with CH₄ + air replenishment, the accumulated concentrations of acetate (4.1 mM), malate (0.02 mM) and propionate (0.07 mM) were significantly higher than those in the control (p value < 0.05) (Fig. 6b, c). In this study, *Methylobacter* sp. S3L5C is hypothesized to convert carbon from CH₄ (C-CH₄) into organic acids, CO₂, and biomass. The carbon conversion into total accumulated organic acids in the test with CH₄ + air replenishment (2.5% of the consumed C-CH₄) was significantly higher than those in the control test (1.2% of the consumed C-CH₄) (p value = 0.037) (Supplementary Table S6). In both experimental conditions, the carbon yields of C-CO₂ and C-biomass derived from C-CH₄ were similar in the range of 42.2–46.3% and 51.1–56.4%, respectively (p value = 0.124) (Supplementary Table S6).

DISCUSSION

Strain S3L5C, isolated and classified in this study as *Methylobacter* sp., has been previously reported to be a dominant genus in the

oxic-anoxic transition zone in boreal and subarctic lakes, ponds, and wetlands [7, 8, 10, 11, 50–52]. Our phylogenetic and phylogenomic tree analyses showed that the isolate represents a ubiquitous cluster of *Methylobacter* spp. in lake and pond ecosystems. The *Methylobacter* sp. S3L5C genome contained genes encoding key enzymes involved in aerobic CH₄ oxidation and organic acid production (fermentative metabolism). According to previous studies and MAG analyses of this study, the genetic potential of *Methylobacter* spp. for organic acid production is widely dispersed in CH₄-rich aquatic systems (Supplementary Table S5) [7, 10, 25]. Whether or not *Methylobacter* sp. S3L5C is a new species of *Methylobacter*, or a type strain of the previously described *Methylobacter psychrophilus* Z-0021 could not be validated as the strain Z-0021, and its genome is not available. Nevertheless, *Methylobacter* sp. S3L5C represents psychrophilic methanotrophs that rarely exist as isolates.

Organic acid production in MOB is an energy conservation mechanism where pyruvate is oxidized to fermentative by-products instead of biomass formation during substrate-limiting conditions (e.g., CH₄ and O₂) [12, 53]. In our study, the average O₂/CH₄ uptake ratio during incubation from days 4 to 33 (O₂/CH₄ uptake ratio of 1.0 ± 0.5; Supplementary Fig. S4) was lower than the stoichiometric ratio in aerobic CH₄ oxidation (Eq. 1).



These conditions probably induced CH₄ oxidation with O₂ limited amount in the system and initiated the accumulation of

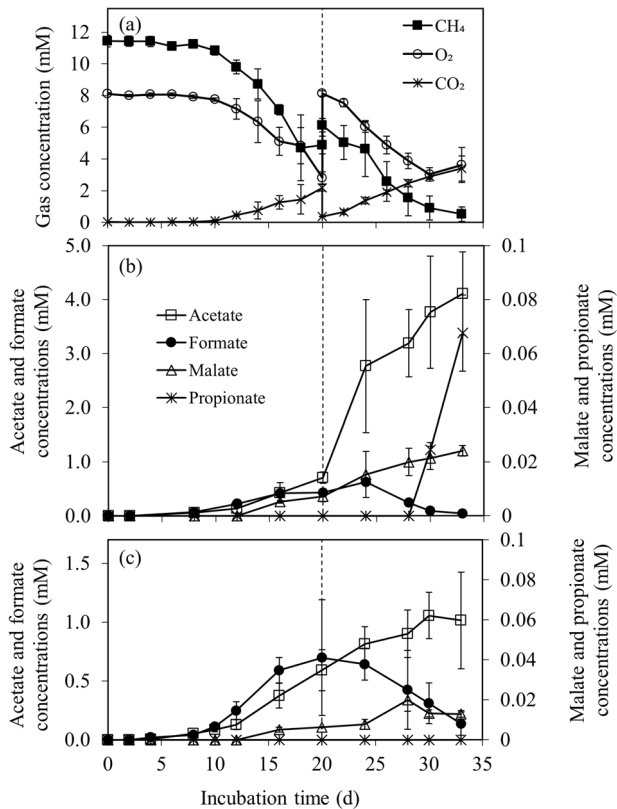


Fig. 6 Potential for organic acid production of *Methylobacter* sp. S3L5C. The profiles of (a) gas composition in the headspace of the test with 20% CH₄ and 80% air replenishment on day 20 and concentrations of organic acids in the liquid medium during 33-day cultivation (b) with and (c) without the replenishment. Error bars indicate the standard deviation of triplicate samples (See Supplementary Table S9 for the dataset).

acetate, propionate, and malate. The O₂/CH₄ uptake behavior was similar to the previous studies conducted using *Methylobacterium buryatense* 5GB1C cultivated under O₂ and CH₄ limitation conditions (O₂/CH₄ uptake ratio of 1.1–1.6) [54, 55].

When *Methylobacter* sp. S3L5C grew in batch cultivation, acetate was observed as the dominant metabolite, and its concentration was remarkably elevated under the conditions with CH₄ + air replenishment in the headspace. *Methylobacter* sp. S3L5C genome lacks the genes encoding phosphate acetyltransferase (*pta*) and pyruvate dehydrogenase (*poxB*). Nevertheless, experimental validation on the metabolite production suggests that the acetate synthesis route might be catalyzed by acetyl-CoA synthetase and ligase from acetyl-CoA found in the genome (*acs* and *acdAB*; Fig. 5 and Supplementary Table S4) [56]. To the best of our knowledge, this is the first study to report the capacity of a MOB isolate to produce propionate, a liquid metabolite commonly produced by archaea and facultative anaerobic bacteria under anaerobic/microaerobic conditions [57–59]. Genes encoding propionate production (*acdAB*, *acs*, and *ackA*) were found in the annotated genome of *Methylobacter* sp. S3L5C. Thus, based on the in silico data (Fig. 5; Supplementary Table S4), we hypothesize that the propionate production from *Methylobacter* sp. S3L5C may occur via succinate and citramalate pathways similar to other propionate-producing microorganisms [58]. Formate accumulation in the liquid culture has been observed during unbalanced growth conditions (e.g., under O₂ limitation and cultivated in methanol as a carbon source) [12, 54, 60]. However, in our study, formate was observed as an intermediate metabolite which was eventually depleted during the cultivation period (Fig. 6b, c).

Although the genes encoding succinate dehydrogenase were annotated in the genome, succinate was not detected in any studied conditions.

While some MOB are capable of nitrogen fixation, ammonium and nitrate are widely used as nitrogen sources for MOB biomass assimilation [18, 61]. Our results revealed the effect of different nitrogen sources (i.e., nitrate and ammonium) on *Methylobacter* sp. S3L5C growth. The strain favored ammonium for biomass assimilation, resulting in a significantly higher growth rate than the nitrate medium (Fig. 3b). The efficient growth in the ammonium medium can be attributed to the original lake environment (high ammonium content, DO < 0.3 mg l⁻¹, Supplementary Fig. S1) from which *Methylobacter* sp. S3L5C was isolated. In the previous study on the bacterial community in anoxic brackish groundwater enrichments, *Methylobacter* sp. was observed as a predominant methanotroph in the CH₄ and ammonium-rich medium, but it was absent in the nitrate-supplemented medium [62]. However, studies on different gamma- and alphaproteobacterial MOB have reported varying responses to the use of nitrate or ammonium as the optimum nitrogen source [13, 60]. For instance, Tays et al. [60] reported that a medium containing ammonium was optimal for the growth of *Methylocystis* sp. Rockwell, albeit with lower lipid content (fatty acid methyl ester, FAME) compared to the growth in nitrate medium [60]. In some circumstances, nitrate favored the growth of *Methylomonas denitrificans* FJG1 under O₂-limited conditions [13]. In our study, the strain's biomass collected from the ammonium medium had significantly less carbohydrate (sugar) content than the cells growing on the nitrate medium (Fig. 3d). This result suggests that the use of different nitrogen sources can be adopted as a strategy to target the major biomass composition (protein, lipid, and carbohydrate contents) during *Methylobacter* sp. S3L5C cultivation. In methanotrophic biomass, carbohydrate commonly represents a carbon sink which might not be preferable for biotechnological applications (e.g., single cell protein and microbial lipid-derived fuels) [55, 63, 64].

In conclusion, our results on *Methylobacter* sp. S3L5C and comparative MAG analyses suggest that *Methylobacter* spp. play a key role in mitigating atmospheric CH₄ emissions and synthesizing organic acids in boreal and subarctic aquatic ecosystems. The findings suggest that the organic acids produced by *Methylobacter* spp. could serve as a carbon source for surrounding heterotrophic microorganisms to sustain a functioning ecosystem [14, 65]. Furthermore, *Methylobacter* sp. S3L5C may provide an alternative source of CH₄-derived metabolites for biotechnological applications, especially in cold systems. For example, organic acid-rich spent media can be used to cultivate recombinant heterotrophs to generate value-added compounds [16, 66, 67]. However, further studies on the effect of alternative electron acceptors (e.g., nitrogen oxides) on metabolism and organic acid production of *Methylobacter* sp. S3L5C and process optimizations are required to enhance the production of CH₄-derived products.

DATA AVAILABILITY

The 16S rRNA gene sequence of *Methylobacter* sp. S3L5C is deposited at GenBank under accession number OM479427. The draft genome assembly of *Methylobacter* sp. S3L5C is available at GenBank under accession number CP076024. The raw reads of the genome sequence are deposited in Sequence Read Archive (SRA) data under accession SRR14663858 for short reads and SRR14663859 for long reads. All data generated and analyzed during this study are included in this published paper and its supplementary information files.

REFERENCES

1. Masson-Delmotte V, Zhai P, Pirani A, Connors SL, Péan C, Zhou B, et al. IPCC, 2021: Climate Change 2021: The Physical Science Basis. Contribution of Working Group I to the Sixth Assessment Report of the Intergovernmental Panel on Climate

- Change 2021. Cambridge University Press, Cambridge, United Kingdom and New York, NY, USA. <https://doi.org/10.1017/9781009157896>.
- Saunio M, Stavert AR, Poulter B, Bousquet P, Canadell JG, Jackson RB, et al. The global methane budget 2000–2017. *Earth Syst Sci Data*. 2020;12:1561–623.
 - Wik M, Varner RK, Anthony KW, MacIntyre S, Bastviken D. Climate-sensitive northern lakes and ponds are critical components of methane release. *Nat Geosci*. 2016;9:99–105.
 - Guo M, Zhuang Q, Tan Z, Shurpali N, Juutinen S, Kortelainen P, et al. Rising methane emissions from boreal lakes due to increasing ice-free days. *Environ Res Lett*. 2020;15:064008.
 - Matthews E, Johnson MS, Genovese V, Du J, Bastviken D. Methane emission from high latitude lakes: methane-centric lake classification and satellite-driven annual cycle of emissions. *Sci Rep*. 2020;10:12465.
 - Sieczko AK, Duc NT, Schenk J, Pajala G, Rudberg D, Sawakuchi HO, et al. Diel variability of methane emissions from lakes. *Proc Natl Acad Sci USA* 2020;117:21488–94.
 - Rissanen AJ, Saarela T, Jääntti H, Buck M, Peura S, Aalto SL, et al. Vertical stratification patterns of methanotrophs and their genetic controllers in water columns of oxygen-stratified boreal lakes. *FEMS Microbiol Ecol*. 2021; <https://doi.org/10.1093/femsec/iaa252>.
 - Rissanen AJ, Saareheimo J, Tirola M, Peura S, Aalto SL, Karvinen A, et al. Gammaproteobacterial methanotrophs dominate methanotrophy in aerobic and anaerobic layers of boreal lake waters. *Aquat Microb Ecol*. 2018;81:257–76.
 - Samad MS, Bertilsson S. Seasonal variation in abundance and diversity of bacterial methanotrophs in five temperate lakes. *Front Microbiol*. 2017;8:142.
 - Smith GJ, Angle JC, Solden LM, Borton MA, Morin TH, Daly RA, et al. Members of the Genus *Methylobacter* Are Inferred To Account for the Majority of Aerobic Methane Oxidation in Oxic Soils from a Freshwater Wetland. *MBio*. 2018;10.1128/mBio.00815–18.
 - van Grinsven S, Oswald K, Wehrli B, Jegge C, Zopfi J, Lehmann MF, et al. Methane oxidation in the waters of a humic-rich boreal lake stimulated by photosynthesis, nitrite, Fe(III) and humics. *Biogeosciences*. 2021;18:3087–101.
 - Kalyuzhnaya MG, Yang S, Rozova ON, Smalley NE, Clubb J, Lamb A, et al. Highly efficient methane biocatalysis revealed in a methanotrophic bacterium. *Nat Commun*. 2013;4:2785.
 - Kits KD, Klotz MG, Stein LY. Methane oxidation coupled to nitrate reduction under hypoxia by the Gammaproteobacterium *Methylomonas denitrificans*, sp. nov. type strain FJG1. *Environ Microbiol*. 2015;17:3219–32.
 - Ho A, de Roy K, Thas O, De Neve J, Hoefman S, Vandamme P, et al. The merrier: heterotroph richness stimulates methanotrophic activity. *ISME J*. 2014;8:1945–8.
 - Krause SMB, Johnson T, Karunaratne YS, Fu Y, Beck DAC, Chistoserdova L, et al. Lanthanide-dependent cross-feeding of methane-derived carbon is linked by microbial community interactions. *Proc Natl Acad Sci USA* 2017;114:358–63.
 - Khanongnuch R, Mangayil R, Santala V, Grethe Hestnes A, Marianne Svenning M, Rissanen AJ. Batch Experiments Demonstrating a Two-Stage Bacterial Process Coupling Methanotrophic and Heterotrophic Bacteria for 1-Alkene Production From Methane. *Front Microbiol*. 2022;13:874627.
 - Pieja AJ, Morse MC, Cal AJ. Methane to bioproducts: the future of the bioeconomy? *Curr Opin Chem Biol*. 2017;41:123–31.
 - Strong PJ, Xie S, Clarke WP. Methane as a Resource: Can the Methanotrophs Add value? *Environ Sci Technol*. 2015;49:4001–18.
 - van Grinsven S, Sinninghe Damsté JS, Harrison J, Polerecky L, Villanueva L. Nitrate promotes the transfer of methane-derived carbon from the methanotroph *Methylobacter* sp. to the methylotroph *Methylotenera* sp. in eutrophic lake water. *Limnol Oceanogr*. 2021;66:878–91.
 - Bertoldo C, Grote R, Antranikian G. Extremophiles: Life in Extreme Environments. In: Bittou G, editor. *Encyclopedia of Environmental Microbiology*. 2003. <https://doi.org/10.1002/0471263397.env099>.
 - Trotsenko YA, Khmelenina VN. Aerobic methanotrophic bacteria of cold ecosystems. *FEMS Microbiol Ecol*. 2005;53:15–26.
 - Rissanen AJ, Mangayil R, Svenning MM, Khanongnuch R. Draft genome sequence data of methanotrophic *Methylovulum psychrotolerans* strain S1L and *Methylomonas paludis* strain S2AM isolated from hypoxic water column layers of boreal lakes. *Data Br*. 2021;38:107364.
 - Kumar S, Stecher G, Li M, Nkay C, Tamura K. MEGA X: Molecular Evolutionary Genetics Analysis Across Computing Platforms. *Mol Biol Evol*. 2018;35:1547–9.
 - Buck M, Garcia SL, Fernandez L, Martin G, Martinez-Rodriguez GA, Saareheimo J, et al. Comprehensive dataset of shotgun metagenomes from oxygen stratified freshwater lakes and ponds. *Sci Data*. 2021;8:131.
 - van Grinsven S, Sinninghe Damsté JS, Abdala Asbun A, Engelmann JC, Harrison J, Villanueva L. Methane oxidation in anoxic lake water stimulated by nitrate and sulfate addition. *Environ Microbiol*. 2020;22:766–82.
 - Seemann T. Barrnap: Basic rapid ribosomal RNA predictor. 2014. <https://github.com/tseemann/barrnap>.
 - Wick RR, Judd LM, Gorrie CL, Holt KE. Unicycler: Resolving bacterial genome assemblies from short and long sequencing reads. *PLoS Comput Biol*. 2017; <https://doi.org/10.1371/journal.pcbi.1005595>.
 - Li W, O'Neill KR, Haft DH, DiCuccio M, Chetverin V, Badretdin A, et al. RefSeq: expanding the Prokaryotic Genome Annotation Pipeline reach with protein family model curation. *Nucleic Acids Res*. 2021;49:D1020–D1028.
 - Haft DH, DiCuccio M, Badretdin A, Brover V, Chetverin V, O'Neill K, et al. RefSeq: an update on prokaryotic genome annotation and curation. *Nucleic Acids Res*. 2018;46:D851–D860.
 - Tatusova T, DiCuccio M, Badretdin A, Chetverin V, Nawrocki EP, Zaslavsky L, et al. NCBI prokaryotic genome annotation pipeline. *Nucleic Acids Res*. 2016;44:6614–24.
 - Kanehisa M, Sato Y, Kawashima M. KEGG mapping tools for uncovering hidden features in biological data. *Protein Sci*. 2022;31:47–53.
 - Aramaki T, Blanc-Mathieu R, Endo H, Ohkubo K, Kanehisa M, Goto S, et al. KofamKOALA: KEGG Ortholog assignment based on profile HMM and adaptive score threshold. *Bioinformatics*. 2020;36:2251–2.
 - Asnicar F, Thomas AM, Beghini F, Mengoni C, Manara S, Manghi P, et al. Precise phylogenetic analysis of microbial isolates and genomes from metagenomes using PhyloPhlAn 3.0. *Nat Commun*. 2020;11:2500.
 - Stamatakis A. RAxML version 8: a tool for phylogenetic analysis and post-analysis of large phylogenies. *Bioinformatics*. 2014;30:1312–3.
 - Seemann T. Prokka: rapid prokaryotic genome annotation. *Bioinformatics*. 2014;30:2068–9.
 - Jain C, Rodriguez-R LM, Phillippy AM, Konstantinidis KT, Aluru S. High throughput ANI analysis of 90K prokaryotic genomes reveals clear species boundaries. *Nat Commun*. 2018;9:5114.
 - Meier-Kolthoff JP, Göker M. TYGS is an automated high-throughput platform for state-of-the-art genome-based taxonomy. *Nat Commun*. 2019;10:2182.
 - Okonkwo O, Lakaniemi A-M, Santala V, Karp M, Mangayil R. Quantitative real-time PCR monitoring dynamics of *Thermotoga neapolitana* in synthetic co-culture for biohydrogen production. *Int J Hydrogen Energy*. 2018;43:3133–41.
 - Masuko T, Minami A, Iwasaki N, Majima T, Nishimura S-I, Lee YC. Carbohydrate analysis by a phenol-sulfuric acid method in microplate format. *Anal Biochem*. 2005;339:69–72.
 - Omel'chenko MV, Vasil'eva LV, Zavarzin GA, Savel'eva ND, Lysenko AM, Mityushina LL, et al. A Novel Psychrophilic Methanotroph of the Genus *Methylobacter*. *Microbiol*. 1996;65:339–43.
 - Wartiainen I, Hestnes AG, McDonald IR, Svenning MM. *Methylobacter tundripaludum* sp. nov., a methane-oxidizing bacterium from Arctic wetland soil on the Svalbard islands, Norway (78° N). *Int J Syst Evol Microbiol*. 2006;56:109–13.
 - Goris J, Konstantinidis KT, Klappenbach JA, Coenye T, Vandamme P, Tiedje JM. DNA-DNA hybridization values and their relationship to whole-genome sequence similarities. *Int J Syst Evol Microbiol*. 2007;57:81–91.
 - Khatiri K, Mohite J, Pandit P, Bahuliker RA, Rahalkar MC. Isolation, Description and Genome Analysis of a Putative Novel *Methylobacter* Species (*Ca. Methylobacter col?*) Isolated from the Faeces of a Blackbuck (Indian Antelope). *Microbiol Res*. 2021;12:513–23.
 - Kim M, Oh HS, Park SC, Chun J. Towards a taxonomic coherence between average nucleotide identity and 16S rRNA gene sequence similarity for species demarcation of prokaryotes. *Int J Syst Evol Microbiol*. 2014;64:346–51.
 - Luo C, Rodriguez-R LM, Konstantinidis KT. MyTaxa: An advanced taxonomic classifier for genomic and metagenomic sequences. *Nucleic Acids Res*. 2014; <https://doi.org/10.1093/nar/gku169>.
 - Orata FD, Meier-Kolthoff JP, Sauvageau D, Stein LY. Phylogenomic Analysis of the Gammaproteobacterial Methanotrophs (order *Methylococcales*) Calls for the Reclassification of Members at the Genus and Species Levels. *Front Microbiol*. 2018;9:3162.
 - Stackebrandt E, Ebers J. Taxonomic parameters revisited: tarnished gold standards. *Microbiol Today*. 2006;33:152–5.
 - Mohammadi SS, Pol A, van Alen T, Jetten MSM, Op den Camp HJM. Ammonia Oxidation and Nitrite Reduction in the Verrucomicrobial Methanotroph *Methylophilum fumarolicum* SolV. *Front Microbiol*. 2017;8:1901.
 - Versantvoort W, Pol A, M Jetten MS, Van NL, Reimann J, Kartal B, et al. Multiheme hydroxylamine oxidoreductases produce NO during ammonia oxidation in methanotrophs. *Proc Natl Acad Sci USA* 2020;117:24459–63.
 - Cabrol L, Thalasso F, Gandois L, Sepulveda-Jauregui A, Martinez-Cruz K, Teisserenc R, et al. Anaerobic oxidation of methane and associated microbiome in anoxic water of Northwestern Siberian lakes. *Sci Total Environ*. 2020;736:139588.
 - Cassarini C, Rene ER, Bhattarai S, Vogt C, Musat N, Lens PNL. Anaerobic methane oxidation coupled to sulfate reduction in a biotrickling filter: Reactor performance and microbial community analysis. *Chemosphere*. 2019;236:124290.
 - Martin G, Rissanen AJ, Garcia SL, Mehrshad M, Buck M, Peura S. *Candidatus Methylophilus* Drives Peaks in Methanotrophic Relative Abundance in Stratified Lakes and Ponds Across Northern Landscapes. *Front Microbiol*. 2021;12:669937.
 - Lee OK, Hur DH, Nguyen DTN, Lee EY. Metabolic engineering of methanotrophs and its application to production of chemicals and biofuels from methane. *Biofuels Bioprod Biorefining*. 2016;10:848–63.

54. Gilman A, Fu Y, Hendershott M, Chu F, Puri AW, Smith AL, et al. Oxygen-limited metabolism in the methanotroph *Methylobacterium buryatense* 5GB1C. PeerJ. 2017; <https://doi.org/10.5281/zenodo.842900>.
55. Gilman A, Laurens LM, Puri AW, Chu F, Pienkos PT, Lidstrom ME. Bioreactor performance parameters for an industrially-promising methanotroph *Methylobacterium buryatense* 5GB1. Microb Cell Fact. 2015;14:182.
56. Schäfer T, Selig M, Schönheit P. Acetyl-CoA synthetase (ADP forming) in archaea, a novel enzyme involved in acetate formation and ATP synthesis. Arch Microbiol. 1993;159:72–83.
57. Baleeiro FCF, Ardila MS, Kleinstaub S, Sträuber H. Effect of Oxygen Contamination on Propionate and Caproate Formation in Anaerobic Fermentation. Front Bioeng Biotechnol. 2021;9:725443.
58. Gonzalez-Garcia RA, McCubbin T, Navone L, Stowers C, Nielsen LK, Marcellin E. Microbial propionic acid production. Fermentation. 2017;3:21.
59. Moreira JPC, Diender M, Arantes AL, Boeren S, Stams AJM, Alves MM, et al. Propionate Production from Carbon Monoxide by Synthetic Cocultures of Acetobacterium wieringae and Propionigenic Bacteria. Appl Environ Microbiol. 2021; <https://doi.org/10.1128/AEM.02839-20>.
60. Tays C, Guarnieri MT, Sauvageau D, Stein LY. Combined Effects of Carbon and Nitrogen Source to Optimize Growth of Proteobacterial Methanotrophs. Front Microbiol. 2018;9:2239.
61. Hanson RS, Hanson TE. Methanotrophic Bacteria. Microbiol Rev. 1996;60:439–71.
62. Kutvonen H, Rajala P, Carpén L, Bomberg M. Nitrate and ammonia as nitrogen sources for deep subsurface microorganisms. Front Microbiol. 2015;6:1079.
63. Fei Q, Puri AW, Smith H, Dowe N, Pienkos PT. Enhanced biological fixation of methane for microbial lipid production by recombinant *Methylobacterium buryatense*. Biotechnol Biofuels. 2018;11:129.
64. Nguyen AD, Lee EY. Engineered Methanotrophy: a Sustainable Solution for Methane-Based Industrial Biomanufacturing. Trends Biotechnol. 2021;39:381–96.
65. Kankaala P, Huotari J, Peltomaa E, Saloranta T, Ojala A. Methanotrophic activity in relation to methane efflux and total heterotrophic bacterial production in a stratified, humic, boreal lake. Limnol Oceanogr. 2006;51:1195–204.
66. Lee H, Baek JI, Lee JY, Jeong J, Kim H, Lee DH, et al. Syntrophic co-culture of a methanotroph and heterotroph for the efficient conversion of methane to mevalonate. Metab Eng. 2021;67:285–92.
67. Takeuchi M, Yoshioka H. Acetate excretion by a methanotroph, *Methylocaldum marinum* S8, under aerobic conditions. Biosci Biotechnol Biochem. 2021;85:2326–33.
68. Bowman JP, McCammon SA, Skerratt JH. *Methylosphaera hansonii* gen. nov., sp. nov., a psychrophilic, group I methanotroph from Antarctic marine-salinity, meromictic lakes. Microbiology. 1997;143:1451–9.

ACKNOWLEDGEMENTS

This research work was funded by the Kone foundation [grant number 201803224 for AJR and RK] and the Academy of Finland [grant number 323214 for RM]. The authors thank Anne Grethe Hestnes, The Arctic University of Norway, Tromsø, Norway, for her

guidance and support in methanotroph isolation and cultivation. The authors also thank the staff at Lammi Biological Station (Finland) for their support in sampling.

AUTHOR CONTRIBUTIONS

RK performed experiments and analyses and wrote the original draft. RK, RM, and AJR conceived and designed the study. RK, RM, and AJR contributed data analysis. RM, MMS, and AJR supervised the work. AJR and RK performed bioinformatic analysis. All authors reviewed and edited the paper.

COMPETING INTERESTS

The authors declare no competing interests.

ADDITIONAL INFORMATION

Supplementary information The online version contains supplementary material available at <https://doi.org/10.1038/s43705-022-00172-x>.

Correspondence and requests for materials should be addressed to Ramita Khanongnuch or Antti Juhani Rissanen.

Reprints and permission information is available at <http://www.nature.com/reprints>

Publisher's note Springer Nature remains neutral with regard to jurisdictional claims in published maps and institutional affiliations.



Open Access This article is licensed under a Creative Commons Attribution 4.0 International License, which permits use, sharing, adaptation, distribution and reproduction in any medium or format, as long as you give appropriate credit to the original author(s) and the source, provide a link to the Creative Commons license, and indicate if changes were made. The images or other third party material in this article are included in the article's Creative Commons license, unless indicated otherwise in a credit line to the material. If material is not included in the article's Creative Commons license and your intended use is not permitted by statutory regulation or exceeds the permitted use, you will need to obtain permission directly from the copyright holder. To view a copy of this license, visit <http://creativecommons.org/licenses/by/4.0/>.

© The Author(s) 2022